

Electronic Entanglement in the Vicinity of a Superconductor

Gordey B. Lesovik^{a,b,c}, Thierry Martin^b, and Gianni Blatter^c

^a*L.D. Landau Institute for Theoretical Physics, Russian Academy of Sciences, Kosyginna Str. 2, 117940, Moscow*

^b*Centre de Physique Théorique et Université de la Méditerranée, Case 907, 13288 Marseille, France*

^c*Theoretische Physik, ETH-Hönggerberg, CH-8093 Zürich, Switzerland*

(December 2, 2024)

A weakly biased normal-metal–superconductor junction is considered as a potential device where entangled pairs of quasi-particles are injected into the normal metallic lead. These two-particle states arise from Cooper pairs decaying into the normal lead and are characterized by entangled spin- and orbital degrees of freedom. Two EPR–type experiments are proposed to probe this entanglement via the measurement of the current–current cross-correlator between two normal leads arranged in a fork geometry, using either spin- or momentum filters.

PACS 03.67.Hk,72.70.+m,74.50.+r

The nonlocal nature of quantum mechanics has been demonstrated theoretically [1] using entangled pairs of particles several decades ago. Recently, potential applications of this entanglement have been found in quantum cryptography [2], in quantum teleportation [3], and in quantum computing [4]. Indeed, entangled pairs of quantum bits (q-bits) are essential elements of such quantum cryptographical schemes and quantum computing algorithms. It is thus necessary to search for practical ways to produce such pairs given a specific interaction between particles. While past experiments have focused on pairs of photons [5] propagating in vacuum, attention is now turning to electronic systems [6], where this entanglement interaction can be stronger. In particular, mesoscopic conductors present the advantage that coherence can be achieved over appreciable distances. A scheme was recently presented [7] which discussed the entanglement of electrons via the exchange interaction in pairs of quantum dots. Here, we propose a rather robust electronic entanglement scheme based on the Andreev reflection of electrons and holes at the boundary between a normal metal and a superconductor.

The basic concept underlying the microscopic description of superconductivity is the formation of Cooper pairs. A normal metal in close vicinity to a superconductor bears the trace of this phenomenon through the presence of Bogoliubov quasi-particles, or, in Green’s function language, through the non-vanishing of the Gor’kov function [8] $F = \langle c_{\mathbf{k}\uparrow} c_{-\mathbf{k}\downarrow} \rangle$ ($c_{\mathbf{k}\sigma}$ denote the usual electron creation operators). While in a superconductor $F = \Delta/\lambda$ is a consequence of a nonzero gap parameter Δ (λ is the pairing potential), the coherence surviving in the adjacent normal metal can be understood through the presence of evanescent Cooper pairs. These decaying Cooper pairs involve two electrons with entangled spin- and orbital degrees of freedom, carrying opposite spins in the case of usual s -wave pairing, and with kinetic energies above and below the superconductor chemical potential. This so-called proximity effect has been illustrated by

several recent experiments [9].

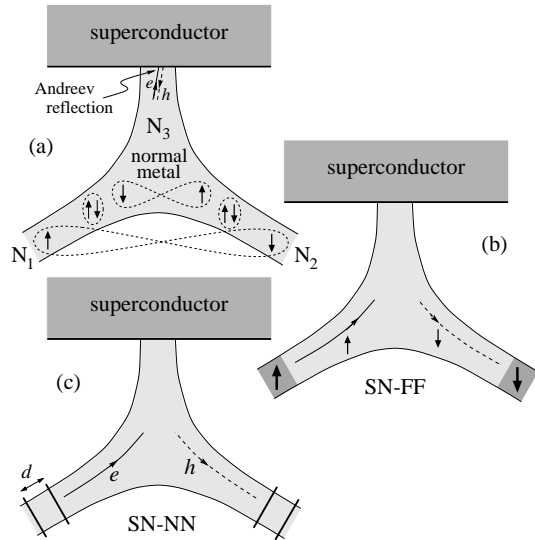


FIG. 1. Normal-metal–superconductor (NS) junction with the normal-metal lead arranged in a fork geometry. (a) Without filters, entangled pairs of quasi-particles (Cooper pairs) injected into the lead N_3 propagate into leads N_1 or N_2 either as a whole or one by one. The ferromagnetic filters in setup (b) enforce the separation of the entangled spins, while the Fabry-Perot type interferometers in the setup (c) separate electron- and hole type quasiparticles.

In order to detect this entanglement and implement it for applications, it is necessary to achieve a spatial separation between the two constituent electrons. The entanglement apparatus which is proposed here consists of a mesoscopic normal-metal–superconductor (NS) junction with normal leads arranged in a fork geometry (see Fig. 1). Using appropriate spin- or energy filters in the two normal leads, the entanglement of quasi-particle pairs can be quantified in an EPR type experiment through a comparison of the intra- and inter- lead noise.

The current noise in a plain SN-NN fork geometry – without selective filters at the normal probes – has been considered in Ref. [10] to explore the possibility of posi-

tive noise correlations. The resulting current correlations are due to paired electrons penetrating the two normal leads both jointly and separately (see Fig. 1(a)). The latter processes are the most relevant for observing entanglement, so that additional scattering elements need to be added on the normal side to prohibit the penetration of the entire pair in a given lead. Below two distinct schemes for achieving this are discussed: a) using two ferromagnetic metal contacts (with magnetizations in opposite directions) in each lead (Fig. 1b) which effectively block propagation of the opposite spin, b) exploiting the difference in kinetic energies of electron and hole quasi-particles and thus positioning Fabry Perot type energy filters (Fig. 1c) on the normal leads which select energies symmetrically above and below the superconducting chemical potential. In both proposals, the penetration of a full pair into a given lead is prohibited, while allowing the split pair to pass the filters with one (say, spin ‘up’) electron propagating through one lead and the other (spin ‘down’) electron through the second lead.

A step like dependence of the gap parameter at the interface is assumed, subgap transport is specified, while the normal leads are ballistic. Using the scattering formulation of NS transport [11], the current operator per spin in normal lead n is defined as:

$$I_{\sigma n}(t) = \frac{ie\hbar}{2m} \sum_{\alpha, \alpha'} \int_0^\infty d\varepsilon d\varepsilon' \{ [u_{\varepsilon\alpha}^*(x) \overset{\leftrightarrow}{\partial}_x u_{\varepsilon'\alpha'}(x)] \gamma_{\varepsilon\alpha}^\dagger \gamma_{\varepsilon'\alpha'} - [v_{\varepsilon\alpha}^*(x) \overset{\leftrightarrow}{\partial}_x v_{\varepsilon'\alpha'}(x)] \gamma_{\varepsilon'\alpha'} \gamma_{\varepsilon\alpha}^\dagger \} \exp[i(\varepsilon - \varepsilon')t], \quad (1)$$

where the operators $\gamma_{\varepsilon\alpha}$ describe electron and hole Bogoliubov quasiparticles (with positive energies ε) on the normal side with $\alpha = \{p, \sigma, n\}$ a multi-index characterizing the ‘charge’ p ($= e, h$), spin σ ($= \pm 1/2$), and incidence (lead n); $f \overset{\leftrightarrow}{\partial}_x g \equiv f\partial_x g - g\partial_x f$. The associated wave functions ($u_{\varepsilon\alpha}(x)$ and $v_{\varepsilon\alpha}(x)$) are expressed in terms of the scattering matrix. As an example, for an electron with spin σ incident from lead n and observed in lead m (at a position x_m):

$$u_{\varepsilon e \sigma n}(x_m) \simeq [\delta_{nm} e^{ik_+ x_n} + s_{e\sigma n, e\sigma m} e^{-ik_+ x_m}] / \sqrt{hv_+}, \quad (2)$$

$$v_{\varepsilon e \sigma n}(x_m) \simeq [s_{e\sigma n, h-\sigma m} e^{ik_- x_m}] / \sqrt{hv_-}, \quad (3)$$

with wave numbers $k_\pm = \sqrt{2m(\mu_s \pm \varepsilon)}$ and the quasi-particle velocities $v_\pm = \hbar k_\pm / m$ (μ_s is the chemical potential in the superconductor). The difference between the two wave numbers k_\pm will be neglected when appropriately assuming $\mu_s \gg \Delta$. The zero frequency noise correlator $\langle\langle I_{\sigma m} I_{-\sigma n} \rangle\rangle \equiv \int dt \langle\langle I_{\sigma m}(t) I_{-\sigma n}(0) \rangle\rangle$, is the quantity which probes entanglement. Here $\langle\langle \dots \rangle\rangle$ means that the product of the average currents has been subtracted.

The starting point is first to note that for a single channel NS wire, the zero frequency fluctuations of the cur-

rents carried by electrons with different spins are completely correlated,

$$\langle\langle I_\sigma I_{-\sigma} \rangle\rangle = \langle\langle I_\sigma I_\sigma \rangle\rangle, \quad (4)$$

hence $\langle\langle (I_\sigma - I_{-\sigma})^2 \rangle\rangle = 0$. This perfect correlation in the (subgap) motion of the quasi-particles with different spins is a consequence of the entanglement of the Cooper pairs injected into the normal wire.

Next, consider the fork geometry of Fig. 1. For simplicity, single-channel leads are considered in each normal arm labelled N_1 and N_2 , while lead N_3 is terminated with the NS interface. The scattering matrix $s_{\alpha, \alpha'}$ accounts for all scattering processes: a) Andreev reflection at the N_3S interface, the presence of the beam splitter $N_3 \longleftrightarrow N_1, N_2$, and the presence of the spin or energy filters in the leads N_1 and N_2 . Because of the presence of the filters, this device is essentially a two terminal one where electrons with a given spin from lead 1 are converted into holes with an opposite spin in lead 2. The correlations between 1 and 2 can then be obtained using the definitions of both Eq. (1) and the noise:

$$\langle\langle I_{\sigma 1} I_{-\sigma 2} \rangle\rangle = \frac{e^2}{h} \sum_{\alpha, \alpha'} \int_0^{eV_1} d\varepsilon |s_{\alpha, \alpha'}|^2 (1 - |s_{\alpha, \alpha'}|^2) \quad (5)$$

when a voltage eV_1 is imposed between the lead N_1 and the superconductor, while keeping the lead N_2 unbiased. Eq. (5) is derived at zero temperature, assuming sharp Fermi functions for the electron and holes incident from the two normal terminals. For the case of ferromagnetic filters, the chemical potential which enters these distributions depends also on the spin index. The multi-indices α and α' to be summed over in (5) depend on the type of filters in the normal leads N_1 and N_2 : For ferromagnetic filters (SN-FF) with the spin in $F_{1(2)}$ pointing up (down) $\alpha = \{e(h) \uparrow 1\}$ and $\alpha' = \{h(e) \downarrow 2\}$ (the propagation of other states is blocked by the filters). On the other hand, for the setup selecting a definite quasi particle energy via Fabry-Perot type filters we have to sum over spins with $\alpha = \{e \uparrow (\downarrow) 1\}$ and $\alpha' = \{h \downarrow (\uparrow) 2\}$ (we assume filters selecting quasi particles and quasi holes in leads N_1 and N_2 , respectively). Applying the same voltage to the lead N_2 as well does not change the answer in the normal fork (SN-NN) but renders the result for the ferromagnetic filters (SN-FF) twice larger.

The result of Eq. (5), together with the fact that the two currents with opposite spin in the two arms of the fork are necessarily correlated, constitutes the main justification for this proposed entanglement detection apparatus. Indeed, Eq. (5) corresponds precisely to the current noise in lead 1.

To complete this scheme, $s_{\alpha, \alpha'}$ are expressed in terms of the transmission and reflection amplitudes t_{13}, t_{23} , and r_{ii} , ($i = 1, 2$) on the normal side [12]. At this stage, it seems unnecessary to provide a realistic description of the device, given the number of parameters which describe

it in practice. The iterative scheme of Fig. 2 which accounts for all interference processes in a device which is composed of individual “blocks”, provides the general framework for potential applications. The Andreev reflection amplitude for an electron incident from N_1 then reads:

$$|s_{e\sigma 1,h-\sigma 2}|^2 = \frac{|t_{13+}|^2 |t_{23-}|^2}{1 + |r_{11+}|^2 |r_{22-}|^2 + 2\text{Re}(r_{33+}r_{33-}^*)}. \quad (6)$$

where the indices \pm indicate that the energy dependent scattering amplitudes have to be evaluated at the positive(negative) value of the quasi particle energy $\varepsilon(-\varepsilon)$. For each energy ε only one of the two leads, N_1 or N_2 , is open, resulting in a two-terminal device, thus the relations $|r_{ii}|^2 = 1 - |t_{ii}|^2 = |r_{33}|^2$ hold. The main feature contained in Eq. (6) are the Andreev type resonances building up within the normal-metal leads. These resonances are determined through the sign changes in $\text{Re}(r_{33+}r_{33-}^*)$ and their distance $\sim \hbar v_F/L$ is determined via the Fermi velocity v_F and the characteristic size L of the region. In addition, zeros appear in the spectral density which are a consequence of a vanishing transmission for electrons or holes in this three lead geometry. The building blocks of this device are now analyzed:

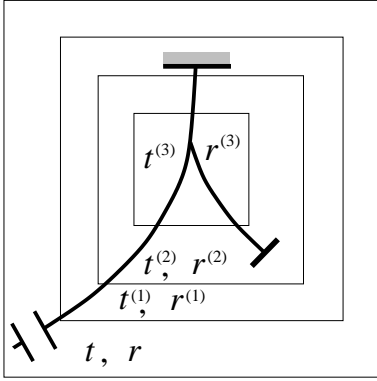


FIG. 2. The scattering amplitudes t and r determining the noise correlator (5) incorporate all the internal scattering features of the fork, the beam splitter ($\rightarrow t^{(3)}, r^{(3)}$), the stubs ($\rightarrow t^{(2)}, r^{(2)}$), the normal scattering at the NS interface ($\rightarrow t^{(1)}, r^{(1)}$), and the filters ($\rightarrow t, r$).

Beam Splitter: Time reversal invariance is assumed for simplicity. It is then possible to express the transmission probability, say, between 1 and 2 in terms of the other two transmissions:

$$T_{12}^{(3)} = \frac{T_{13}^{(3)} T_{23}^{(3)}}{T_{\Sigma}^{(3)2}} \left[2 - T_{\Sigma}^{(3)} \pm 2\sqrt{1 - T_{\Sigma}^{(3)}} \right], \quad (7)$$

where $T_{\Sigma}^{(3)} \equiv T_{13}^{(3)} + T_{23}^{(3)}$, and $T_{ij}^{(3)} = |t_{ij}^{(3)}|^2$. For a fully symmetric beam splitter $T_{ij}^{(3)} = 4/9$. A partially symmetric setup (with respect to the leads N_1, N_2) with small transmissions $T_{23}^{(3)} = T_{13}^{(3)}$ has been studied in Ref. [13].

The choice of the lower sign in (7) allows us to consider also the case when all three transmissions are small, so this parametrization allows to explore the whole range of splitter transmission. Using the unitarity of the scattering matrix, the reflection amplitudes of the splitter are then specified:

$$r_{ii}^{(3)} = t_{jk}^{(3)*} t_{ij}^{(3)} t_{ik}^{(3)} \left[\frac{1}{2T_{jk}^{(3)}} - \frac{1}{2T_{ij}^{(3)}} - \frac{1}{2T_{ik}^{(3)}} \right]. \quad (8)$$

The phases of the reflection and transmission amplitudes, in addition to describing the intrinsic properties of the links between the three wires, account for the choice of the origin in each lead. Practical choices for these origins are: a) the position of the NS interface in lead N_3 and b) that of the filters in N_1 and N_2 . Typical phases accumulated during free propagation are $\exp(\pm ik_{\pm}b)$ with b a typical length in the beam splitter.

Stubs: When blocking the propagation through N_2 with a filter, the transmission and reflection amplitudes $t_{13}^{(2)}, r_{33}^{(2)}$, and $r_{11}^{(2)}$ follow from the transmission and reflection amplitudes $t_{12}^{(3)}, t_{13}^{(3)}, t_{23}^{(3)}, r_{11}^{(3)}$, and $r_{22}^{(3)}$ of the three bare leads via

$$t_{13}^{(2)} = \frac{t_{13}^{(3)} - t_{12}^{(3)} t_{23}^{(3)} + t_{13}^{(3)} r_{22}^{(3)}}{1 + r_{22}^{(3)}}, \quad (9)$$

$$r_{33}^{(2)} = -\frac{t_{23}^{(3)}}{1 + r_{22}^{(3)}}, \quad r_{11}^{(2)} = r_{11}^{(3)} - \frac{t_{23}^{(3)2}}{1 + r_{22}^{(3)}}. \quad (10)$$

When blocking occurs at N_1 , the amplitudes are obtained by exchanging in Eqs. (9) and (10) the lead indices.

NS boundary: in the next iteration, an additional normal scattering component at the NS interface has to be accounted for (the Andreev reflection has already been included in (6)). Combining the two scatterers $\{t_{13}^{(2)}, r_{33}^{(2)}, r_{11}^{(2)}\}$ and $\{t_{\text{NS}}, r_{\text{NS}}, r'_{\text{NS}}\}$ in series we obtain the amplitudes at the next level,

$$t_{13}^{(1)} = \frac{t_{13}^{(2)} t_{\text{NS}}}{1 - r_{33}^{(2)} r'_{\text{NS}}}, \quad (11)$$

$$r_{33}^{(1)} = r_{\text{NS}} + \frac{t_{\text{NS}}^2 r_{33}^{(2)}}{1 - r_{33}^{(2)} r'_{\text{NS}}}, \quad r_{11}^{(1)} = r_{11}^{(2)} + \frac{t_{13}^{(2)2} r'_{\text{NS}}}{1 - r_{33}^{(2)} r'_{\text{NS}}}, \quad (12)$$

where the primed reflection amplitude r'_{NS} is associated with the particle incident from the superconductor.

The present scheme fully specifies the scattering matrix $s_{\alpha,\alpha'}$ for the case with ferromagnetic filters (SN-FF). For the case of energy selective filters, the discussion is completed by a description of the Fabry Perot interferometer located at the open lead.

Fabry Perot: The effect of an energy selective filter is accounted for by following the above scheme for the inclusion of the NS barrier, starting with the generation $\{t_{13}^{(1)}, r_{33}^{(1)}, r_{11}^{(1)}\}$ and linking this block in series with the Fabry Perot interferometer characterized through $\{t_{\text{FP}}, r_{\text{FP}}, r'_{\text{FP}}\}$, where

$$t_{\text{FP}} = \frac{t_1 t_2 \exp(ikd)}{1 - r_1 r_2' \exp(2ikd)}, \quad (13)$$

with t_1, t_2, r_1', r_2 the scattering amplitudes characterizing the barriers of the interferometer and d denotes the separation between the barriers (similar expressions are trivially obtained for the reflection coefficients r_{FB} and r'_{FB}). Note that the resonance spacing should be larger than the applied bias for proper device operation as a filter. The initial resonance lines produced by the quantum dot will then be decorated by Andreev-type resonances and zeros originating from the NS-fork structure.

As a corollary, note that the proximity induced entanglement of quasi particles in NS-fork type devices has already been implicit in a transport experiment carried out in Ref. [14], and also suggested in Ref. [15]. For specificity, the above SN-NN setup is considered, with the lead N_1 biased with respect to the superconductor, while keeping the lead N_2 at the chemical potential of the superconductor. As a result, a finite current $I_2(V_1) = (2e/h) \int_0^{eV_1} d\varepsilon |s_{e\uparrow 1, h\downarrow 2}|^2$ will flow through lead N_2 in response to the bias eV_1 across lead N_1 . While both experiments in Ref. [14] use a magnetic field to separate electron- and hole type quasi particles, the more recent suggestion of Ref. [15] proposes two ferromagnetic needles, a setup similar to our SN-FF device. This Andreev drag effect is quite robust and decreases only gradually with decreasing quality of the filters. The condition for this drag effect to persist reads: $\int_0^{eV_1} d\varepsilon [|s_{e\uparrow 1, h\downarrow 2}|^2 - |s_{e\uparrow 1, e\uparrow 2}|^2] > 0$, implying that the normal current injected from lead N_1 to lead N_2 remains smaller than the ‘drag current’ due to Andreev reflected holes. Note that the current I_2 will vanish when replacing the s -wave superconductor with a p -wave material or a normal conductor.

In conclusion, measuring the current cross-correlator in a NS-fork structure allows to probe the proximity-induced entanglement of electrons in an emphatic way and thus provides a solid state analog of the famous EPR experiment usually carried out with photons. Using the special fork geometry with, say, Fabry-Perot filters one arrives at a natural source of spin-entangled electron pairs, a device with potential applications in quantum computing architectures based on spintronics [16]. This device presents the advantage – on its counterpart with ferromagnetic filters – that it can be realized with nowadays splitters [17] and quantum dot technology, with semiconductor-superconductor heterostructures [18]. The formation of sharp resonances in the conductance of the dots is sufficient to achieve this entanglement, without additional coupling between the dots. Moreover, this SN-NN device appears to be more promising regarding potential applications to quantum information processing. The insertion of Fabry-Perot filters

destroys only the orbital entanglement of the electrons, while the (most valuable) spin entanglement persists, contrary to the situation in the SN-FF device where the ferromagnetic filters project the spin.

We thank M. Feigelman and M. Reznikov for useful discussions and the Swiss NSF for financial support. GBL acknowledges support from NWO grant for collaboration with Russia.

- [1] A. Einstein, B. Podolsky, and N. Rosen, Phys. Rev. **47**, 777 (1935).
- [2] A. Ekert, Phys. Rev. Lett. **67**, 661 (1991).
- [3] C.H. Bennett *et al.*, Phys. Rev. Lett. **70**, 1895 (1993).
- [4] A. Steane, Rep. Prog. Phys. **61**, 117 (1998).
- [5] J.F. Glauser and A. Shimony, Rep. Prog. Phys. **41**, 1981 (1978), and references therein; A. Aspect, P. Grangier, and G. Roger, Phys. Rev. Lett. **47**, 460 (1981); see P.G. Kwiat *et al.*, *ibid.* **75**, 4337 (1995) for modern sources of entangled photon pairs.
- [6] G. Burkard, D. Loss, and E. Sukhorukov, Phys. Rev. B **61**, R16303 (2000).
- [7] D. Loss and E.V. Sukhorukov, Phys. Rev. Lett. **84**, 1035 (2000); M.-S. Choi, C. Bruder, and D. Loss, cond-mat/0001011.
- [8] A.A. Abrikosov, L.P. Gor'kov, and I.E. Dzyaloshinski, *Methods of Quantum Field Theory in Statistical Physics* (Prentice-Hall, Englewood Cliffs, N.J., 1963).
- [9] V.T. Petrushov *et al.*, Phys. Rev. Lett. **70**, 347 (1993); *ibid.* **74**, 5268 (1995); A. Dimoulas *et al.*, *ibid.* **74**, 602 (1995); H. Courtois *et al.*, *ibid.* **76**, 130 (1996); F.B. Müller-Allinger *et al.*, *ibid.* **84**, 3161 (2000).
- [10] J. Torrès and T. Martin, Europhys. J. B **12**, 319 (1999).
- [11] M.J.M. de Jong and C.W.J. Beenakker, Phys. Rev. B **49**, 16070 (1994); B.A. Muzykantskii and D.E. Khmelnitskii, *ibid.* **50**, 3982 (1994); M.P. Anantram and S. Datta, *ibid.* **53**, 16 390 (1996); G. Lesovik, T. Martin and J. Torrès, *ibid.* **60**, 11935 (1999).
- [12] G. B. Lesovik, A. L. Fauchère, and G. Blatter, Phys. Rev. B **55**, 3146 (1997); A. L. Fauchère, G. B. Lesovik and G. Blatter, *ibid.* **58**, 11177 (1998).
- [13] Y. Gefen, J. Imry, and R. Landauer, Phys. Rev. Lett. **52**, 139 (1984); M. Büttiker, Y. Imry and M. Ya. Azbel, Phys. Rev. A **30**, 1982 (1984).
- [14] S.I. Bozhko, V.S. Tsoi and S.E. Yakovlev, Pis'ma Zh. Eksp. Teor. Fiz. **36**, 123 (1982) [JETP Lett. **36**, 153 (1982)]; P.A.M. Benistant, H. van Kampen and P. Wyder, Phys. Rev. Lett. **51**, 817 (1983).
- [15] G. Deutscher and D. Feinberg, App. Phys. Lett. **76**, 487 (2000).
- [16] D. Loss and D.P. di Vincenzo, Phys. Rev. A **57**, 120 (1998).
- [17] M. Henny *et al.*, Science **284**, 296 (1999); W. Oliver *et al.*, *ibid.*, 299 (1999).
- [18] H. Takayanagi *et al.*, Phys. Rev. Lett. **75**, 3533 (1995).